Femtosecond Spectroscopy of the Primary Charge Separation in Reaction Centers of *Chloroflexus aurantiacus* with Selective Excitation in the Q_Y and Soret Bands†

Yueyong Xin,‡ Su Lin,§ and Robert E. Blankenship*,‡

Departments of Biology and Chemistry, Washington University, St. Louis, Missouri 63130, and Department of Chemistry & Biochemistry and the Center for the Study of Early Events in Photosynthesis, Arizona State University, Tempe, Arizona 85287

Received: May 20, 2007; In Final Form: August 6, 2007

The primary charge separation and electron-transfer processes of photosynthesis occur in the reaction center (RC). Isolated RCs of the green filamentous anoxygenic phototrophic bacterium *Chloroflexus aurantiacus* were studied at room temperature by using femtosecond transient absorption spectroscopy with selective excitation. Upon excitation in the Q_Y absorbance band of the bacteriochlorophyll (BChl) dimer (P) at 865 nm, a 7.0 ± 0.5 ps kinetic component was observed in the 538 nm region (Q_X band of the bacteriopheophytin (BPheo)), 750 nm region (Q_Y band of the BPheo), and 920 nm region (stimulated emission of the excited-state of P), indicating that this lifetime represents electron transfer from P to BPheo. The same time constant was also observed upon 740 nm or 800 nm excitation. A longer lifetime (300 ± 30 ps), which was assigned to the time of reduction of the primary quinone, Q_A, was also observed. The transient absorption spectra and kinetics all indicate that only one electron-transfer branch is involved in primary charge separation under these excitation conditions. However, the transient absorption changes upon excitation in the Soret band at 390 nm reveal a more complex set of energy and electron-transfer processes. By comparison to studies on the RCs of the purple bacterium *Rhodobacter sphaeroides*, we discuss the possible mechanism of electron-transfer pathway dependence on excitation energy and propose a model of the *Cf. aurantiacus* RC that better explains the observed results.

Introduction

Chloroflexus (Cf.) aurantiacus is a thermophilic, green, filamentous, anoxygenic, photosynthetic bacterium containing peripheral antenna complexes unique to green bacteria (chlorosomes) and a membranous photosynthetic architecture similar to that found in photosynthetic purple bacteria.[1,2] Substantial evidence has shown that following light absorption, energy is transferred sequentially energetically downhill from the chlorosomes to the membranous light-harvesting complex (LH B808-866 complex) via the chlorosome baseplate and, finally, into the reaction center.[3−8] The primary charge separation processes of photosynthesis occur in the reaction center (RC). The RC of *Cf. aurantiacus* is the smallest RC isolated so far, consisting of only two protein subunits, which show homology to the light (L) and medium (M) subunits of the RC of purple bacteria.[9−12] It contains three bacteriopheophytins (BPheos) and three bacteriochlorophylls (BChls), as compared to two BPheos and four BChls in the RC of purple bacteria, such as *Rhodobacter (Rb.) sphaeroides*.[13,14] X-ray structural data are available for the RC of *Rb. sphaeroides* but not for *Cf. aurantiacus*.[15,16] The primary sequence of the two protein subunits;[9−12] spectroscopic evidence,[13,17] including Stark spectroscopy;[18] and EPR measurements[19] lead to the conclusion that in this RC, two of the BChls form a dimer (P) and that the pigments are arranged on two branches analogous to the RC of purple bacteria.[20−22] The overall initial photochemistry in *Cf. aurantiacus* has been shown by early picosecond measurements to be similar to that in purple bacteria, that is, after primary charge separation, the electron is transferred along the A branch to BPheo (H_A) directly or via the accessory BChl (B_A) to Q_A.[3,21] Although there is a clear, albeit weak, homology in the protein primary sequences of the *Cf. aurantiacus* and *Rb. sphaeroides* reaction centers, some key differences might be relevant for the mechanism of charge separation and the extent of its directionality: (1) In the *Rb. sphaeroides* RC, a histidine is found at position 182 in the M subunit, but in the *Cf. aurantiacus* RC, a leucine is at this position, and thus, the pigment coordinated to this amino acid residue is almost certainly a BPheo instead of a BChl. (2) A glutamic acid at position 104 in the L subunit of the *Rb. sphaeroides* RC is hydrogen-bonded to the keto-oxygen of ring V of H_A, but in *Cf. aurantiacus*, there is a glutamine at this position and, thus, no potential H-bond. The protonated glutamic acid is predicted to significantly stabilize the state $P^+H_A^-$, so that its replacement by glutamine should lead to an increased energy of this state.[23] (3) A tyrosine is found at position 210 in the M subunit of the *Rb. sphaeroides* RC. It is within van der Waals distance to P, B_A, and H_A. However, a nonpolar leucine is located in the equivalent position in *Cf. aurantiacus*. From electrostatic calculations and experimental results on site-directed mutants of *Rb. sphaeroides*, this change is expected to affect the energy of $P^+B_A^-$, which is the deciding factor for the mechanism of primary charge separation.[24,25]

The factors controlling the branching of charge separation are not fully understood. Previously, extensive spectroscopic studies in the femtosecond and picosecond time scales have shown that initial electron transfer in the case of low-energy photons excitation occurs from the lowest excited state of P

† Part of the "Sheng Hsien Lin Festschrift".

* Corresponding author. Tel: 1-314-935-7971. Fax: 1-314-935-4432. E-mail: blankenship@wustl.edu.

‡ Washington University.

§ Arizona State University.

10.1021/jp073900b CCC: $37.00
Published on Web 08/23/2007

(P*) to the photoactive BPheo within several picoseconds in the RCs of purple bacteria and *Cf. aurantiacus*.[21,26−27] Recently, it has been shown that the B-branch electron transfer can be realized by varying either the energetics of the cofactors or energy of excitation photons.[28−31] Of the numerous *Rb. sphaeroides* mutants in which electron transfer has been forced to occur along the B-branch, the H(M182)L mutant is particularly interesting, since this changes the *Rb. sphaeroides* protein sequence and pigment composition closer to that of *Cf. aurantiacus*.[29] In this mutant, called the ϕ-mutant, the histidine at M182 was replaced by leucine, resulting in the replacement of BChl at the B_B position by a BPheo (ϕ_B). An electron-transfer yield of 35% was observed from P to ϕ_B without further transfer to H_B. The *Cf. aurantiacus* RC has the same cofactor content as the ϕ-mutant. However, no electron transfer to the BPheo on the B-branch has been observed so far. It is therefore interesting to compare the electron-transfer processes with 390 nm excitation to that obtained after direct excitation of the lower-energy transitions of the BChl in their Q_Y transitions.

Comparison of the bacterial reaction center to other photosynthetic reaction centers reveals that structural symmetry is common to all these systems and has probably been maintained for billions of years.[32] It is the goal of the current study to test the universality of the energetics and mechanism of primary charge separation in bacterial RCs. We have conducted a study on the energy and electron-transfer dynamics in the reaction center of *Cf. aurantiacus*, as compared with the RC of the purple bacterium *Rb. sphaeroides*. Our results reveal that a similar electron-transfer process upon blue light excitation exists in both bacteria. We also discuss how specific interactions among cofactors might influence the pathway of charge separation on the basis of the structural and protein sequence differences.

Materials and Methods

Cell Growth. *Cf. aurantiacus* strain J-10-f1 was cultivated anaerobically for 3 days in a 15-liter fermentor at 55 °C at low-light condition (400 lux) in a modified medium DG as described in ref 13.

Purification of RC of *Chloroflexus*. Reaction centers were prepared by a modification of the procedure described in ref 17. Briefly, the cytoplasmic membranes obtained according to the method in ref 34 were solubilized with 2% LDAO. After ultracentrifugation, the supernatant was loaded onto a Q-Sepharose HP column, and the RC fraction was eluted using a step NaCl gradient. Gel filtration on an S-200 column and anion exchange on a BioRad UNO Q1 column were used for further purification, concentration, and detergent exchange.

Time-Resolved Spectroscopy Measurements. Femtosecond transient absorption spectroscopy at room temperature was performed using a pump−probe setup, and the data were analyzed as described previously.[35,36] Laser pulses of 150 fs duration and 5 nm spectral bandwidth in the Q_Y range at 740, 800, and 865 nm and the Soret band at 390 nm were used. Absorption changes were measured between 460 and 1080 nm on three different timescales. Transient spectra were recorded using probe pulses polarized at the magic angle with respect to the excitation pulses. The excitation pulse intensity was adjusted such that fewer than 15% of the reaction centers were excited per pulse. This corresponded to an approximate pulse energy of 3−5 μJ in a 1−2 mm diameter spot size.

Results and Discussion

The ground state absorption spectra of *Cf. aurantiacus* and *Rb. sphaeroides* RCs are compared in Figure 1A. The two spectra are normalized at 865 nm, which is the ground state absorbance peak of the special pair, P. The most conspicuous feature of the spectrum of *Cf. aurantiacus* RC is the reduced BChl band at ~813 nm and the increased absorption of BPheo near 760 nm, as compared to that from *Rb. sphaeroides*. These features reveal the different pigment contents and interactions in the two RCs. On the basis of spectral and pigment extraction analysis,[13,14] it has been concluded that the RC of *Cf. aurantiacus* contains three BChls and three BPheos and that the 813 nm absorption band is primarily derived from the single monomeric BChl. However, the structural location of this monomeric BChl is still uncertain. In previous studies, on the basis of comparisons of the primary sequences of the two subunits of the *Cf. aurantiacus* RC to that of the *Rb. sphaeroides* RC, it was found that the histidine bound to the B_B site on the B-branch in the *Rb. sphaeroides* RC is leucine in the *Cf. aurantiacus* RC, and thus, it has been suggested[9−12] that the single monomeric BChl is between P and BPheo on the A branch so that the "extra" BPheo is at the B_B site on the B branch. However, this assignment of subunits of RC in *Cf. aurantiacus* depends on the conventional labeling of names of subunits of RCs in which the longer one has been called the M(edium) subunit and the shorter one has been called the L(ight) subunit[12] However, in *Cf. aurantiacus*, the amino acid sequence of subunit M is 306 amino acids and subunit L is 311 amino acids. Thus, the original labeling of subunits of *Cf. aurantiacus* RC may be misleading and perhaps should be revised. We have realigned the sequences (Figure 1B). A phylogenetic tree (Figure 1C) also suggests that the two subunits of the *Cf. aurantiacus* RC are distantly related to that of the purple bacteria. This tree shows the standard grouping of L and M subunits, although the *Cf. aurantiacus* sequences are significantly more diverged as compared to all the purple bacterial sequences. In addition, the topology of the branches of this tree is found to vary depending on the precise alignment and tree reconstruction routine used (data not shown). This analysis leaves open the possibility that the binding amino acid for the B_B site might be a histidine and that for the B_A site, it might be a leucine. Therefore, we suggest that the A branch may contain two BPheos and the single monomeric BChl is located at the B_B position on the B branch. In addition, the previous assignment of the *Cf. aurantiacus* RC cofactors would imply that the absorption spectrum of *Cf. aurantiacus* RC should have features similar to that of the ϕ_B mutant of the *Rb. sphaeroides* RC, which has the same pigment content and configurations.[29] In the ϕ_B mutant, the B_B is replaced by a BPheo, and the longer wavelength wing of the BChl band around 805 nm is missing from the absorption spectrum. But in the *Cf. aurantiacus* RC, the peak of the BChl band is still located at 813 nm. The shorter wavelength absorbance has been assigned to B_A, and the longer wavelength absorbance, to B_B in the purple bacteria RC.[27] If this is the case in the *Cf. aurantiacus* RC, then the replacement could occur in the B_A site rather then B_B site. In contrast, the absorption spectrum of the *Cf. aurantiacus* RC in the Q_Y region of BChl and BPheo is more similar to another mutant where the histidine ligand of B_A is replaced by a leucine.[30] Taken together, these data suggest that the monomeric BChl may be located on the B-branch in the *Cf. aurantiacus* RC. However, since no structural data of the *Cf. aurantiacus* RC are available to date, this proposal must remain only as a possibility. In this report, we investigated the electron-transfer processes generated using different excitation wavelengths by considering both possible locations of this monomeric BChl.

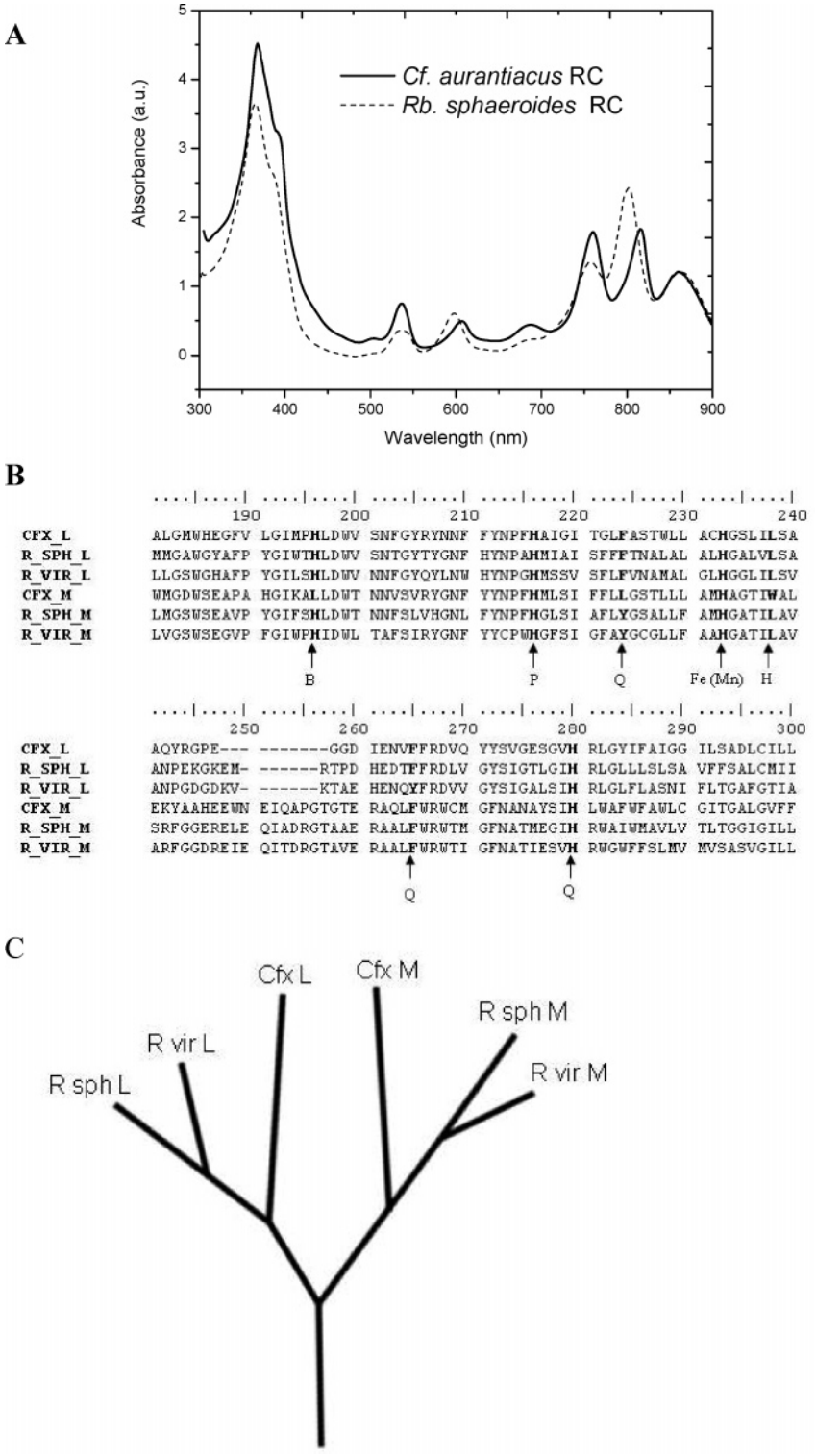

Figure 1. (A) Absorption spectra of *Cf. aurantiacus* (solid line) and *Rb. sphaeroides* (dashed line) bacterial reaction centers, normalized at 865 nm. (B) Partial multiple sequence alignment of the subunits of the RC of *Cf. aurantiacus*, *Rb. sphaeroides*, and *Rhodopseudomonas viridis*. Functionally important residues are identified. (C) Schematic phylogenetic tree of L and M subunits of RCs of *Cf. aurantiacus* and purple bacteria *Rb. sphaeroides* and *Rhodopseudomonas viridis*.

Time-resolved absorption difference spectra of the *Cf. aurantiacus* RC at different delay times in the near-infrared region are shown in Figure 2A and B. Absorption changes in this wavelength region are due to the ground-state bleaching of P together with the stimulated emission of P* between 870 and 1000 nm. The stimulated emission disappears as P* decays to form the charge-separated state, presumably $P^+H_A^-$. The time constant for the formation of primary charge separation is found to be 7.0 ± 0.5 ps, consistent with the results from previous studies.[21,37] As shown in Figure 2A, upon direct excitation of P at 865 nm, there is a broad absorbance decrease centered at 865 nm that becomes gradually larger toward the red wing of the spectra. Following the decay of P*, the true shape of the bleaching of the absorption band of the dimer is revealed in the two longer time spectra shown in Figure 2B. The intermediate time spectra show data acquired at a delay corresponding

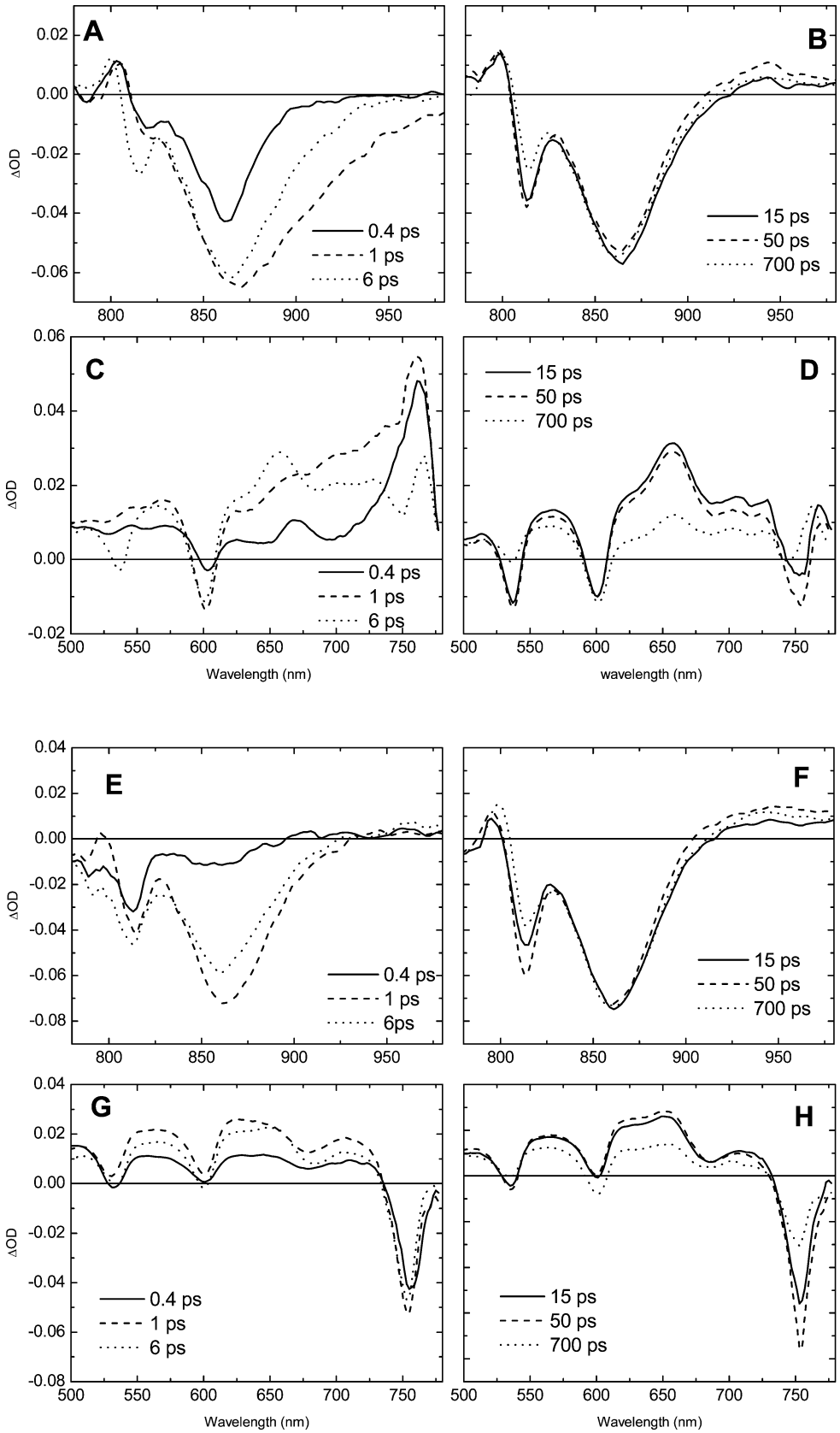

Figure 2. Transient absorption difference spectra of the *Cf. aurantiacus* RC under two excitation conditions. Upon excitation with the low-energy photons at 865 nm, the spectra are illustrated in the infrared region at early time (A) and later time (B) and in the visible region at early time (C) and later time (D), respectively. Upon excitation with the high-energy photons at 390 nm, the corresponding spectra are shown in the panels E−H.

to several P* lifetimes and can be assigned to the state $P^+H_A^-$ on the basis of data in other regions. Similarly, the spectrum at 700 ps dominated by the state $P^+Q_A^-$ formed from the $P^+H_A^-$ state with a time constant of 300 ps. The deduced time constants of electron transfer in the *Cf. aurantiacus* RC are longer than that in the *Rb. sphaeroides* RC.[21,27] This could reflect either a greater distance between P and H_A and between H_A and Q_A or a difference in the energetics for this step in the two types of

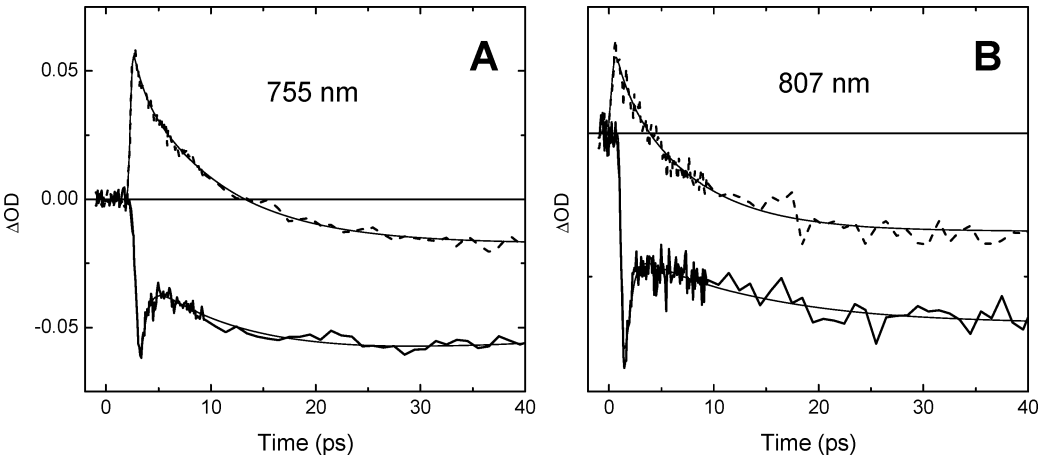

Figure 3. Kinetics of absorbance change at 755 and 807 nm in the *Cf. aurantiacus* RC upon excitation at 865 nm (dashed lines) and 390 nm (solid lines). The smooth lines are the theoretical curves obtained from three-exponential global fitting.

reaction centers, especially if two BPheos are in the A-branch involved in this electron-transfer process. Excitation of B at 800 nm or H at 740 nm resulted in similar time constants for electron-transfer kinetics (data not shown).

The P* spectrum is also characterized by bleaching of the Q_X band of P at 600 nm superimposed on a featureless positive transient absorption (Figure 2C, D). As P* decays, a bleaching band centered near 538 nm in the Q_X band of H_A develops due to the formation of $P^+H_A^-$. The spectrum at 50 ps is dominated by a broad band having a maximum near 665 nm, characteristic of the H_A anion in the state $P^+H_A^-$. The time evolution across the entire 500−770 nm region can be fit with two exponentials with lifetimes of 7 and 300 ps, plus a constant. The spectra at 15 and 50 ps are characteristic of $P^+H_A^-$ and include H_A bleaching near 538 nm and P bleaching near 600 nm. After 700 ps, the bleaching of the Q_X band of H_A has decayed as a result of the electron-transfer process $P^+H_A^- \rightarrow P^+Q_A^-$.

Figure 2E and F shows a series of room temperature transient absorbance change spectra in the Q_Y transition region obtained by excitation of the *Cf. aurantiacus* RCs at 390 nm. With 390 nm excitation, a significant amount of initial bleaching of the ground-state Q_Y absorbance transition of BChl (813 nm) and BPheos (below 760 nm) is formed, and the bleaching persists for at least 2 ps (Figure 2E). No significant P band bleaching is observed until 1 ps after excitation and is followed by a further development between 1 and 6 ps, suggesting that P is not directly excited by 390 nm excitation. The corresponding initial absorption changes of the monomeric BChl and BPheos are also shown in the Q_X region at 600 and 530 nm, respectively (Figure 2G). The BPheos band was centered at 530 nm at 0.4 ps and shifted to 538 nm at later times. A broad absorbance increase around 620 nm also appears at early times and little or no absorbance increase near 660 nm, normally associated with H_A^-. The above data suggest that 390 nm excitation generates a more complex state, probably a mix of excited states of BChl and BPheos and charge-separated states involving BChl and BPheos. At longer times (Figure 2H), the spectra are more similar under the two excitation conditions and indicate that the final state is $P^+Q_A^-$. Kinetic traces at 755 and 807 nm upon 390 nm excitation are compared with those with 865 nm excitation in Figure 3. The striking differences at both wavelengths are the early time bleachings when excited at 390 nm, instead of an excited-state absorption increase when excited at 865 nm. Kinetic traces at 755 (BPheos band, Figure 3A) and 807 nm (BChl band, Figure 3B) show a prompt bleaching followed by a picosecond recovery and a further increase in the bleachings, suggesting the photoactivity of both BChl and BPheos immediately followed by the blue light at 390 nm excitation. The prompt bleaching at 530 nm and absorbance increase near 620 nm suggest a rapid formation of the charge-separated state involving BPheos other than H_A^-. Assignment of this state as a charge-separated state involving B^+ is supported by the fact that excited singlet states of B are known to decay on a time scale of hundreds of femtoseconds due to energy transfer to neighboring cofactors. Because the initial bleaching of H is centered at 530 nm and the corresponding absorption increase is around 620 nm, the comparison with the spectral characteristics of the *Rb. sphaeroides* RC[31] suggests that this initial charge-separated state formed is likely to be $B_B^+H_B^-$. Interestingly, the spectral signatures of the B^+H^- state persist for more than 700 ps (Figure 2H) whereas the same state in the *Rb. sphaeroides* RC lasts less than 10 ps. The spectral differences in the Q_X region between 865 nm excitation and 390 nm excitation remain on the nanosecond time scale, and the profile resembles that of the difference spectrum obtained with 390 nm excitation under the condition that P is oxidized (data not shown). In that case, the only possible long-lived states are BChl*/BPheo* and $B_B^+H_B^-$.

It is also worth mentioning that in the *Cf. aurantiacus* RC, the absorbance changes in the BChl monomer region between 780 and 820 nm show significant differences from that observed in the *Rb. sphaeroides* RC.[26,38] The absorption changes in this region are thought to be the electrochromic shift of the monomeric BChl absorption band at 802 nm due to the formation of $P^+H_A^-$ in the *Rb. sphaeroides* RC.[27,39] The spectral signatures of the electrochromic shift are a broad positive band at 785 nm and a narrow negative band at 810 nm. In contrast, in the *Cf. aurantiacus* RC, the BChl absorption is centered at 813 nm (Figure 1A), and the corresponding absorption changes show positive and negative bands at 795 and 813 nm, respectively. The 795 nm band of the *Cf. aurantiacus* RC is much narrower than that of the 785 nm band of the *Rb. sphaeroides* RC, and the 813 nm band is at exactly the same position as the ground state absorption. One possible reason is that in the *Rb. sphaeroides* RC, both monomeric BChls contribute to the absorption changes in this region due to the oxidation of P. A smaller electrochromic shift is expected in the *Cf. aurantiacus* RC because there is only one monomeric BChl. Another possibility is that the smaller shift of the 813 nm band is due to the fact that the monomeric BChl in the *Cf.*

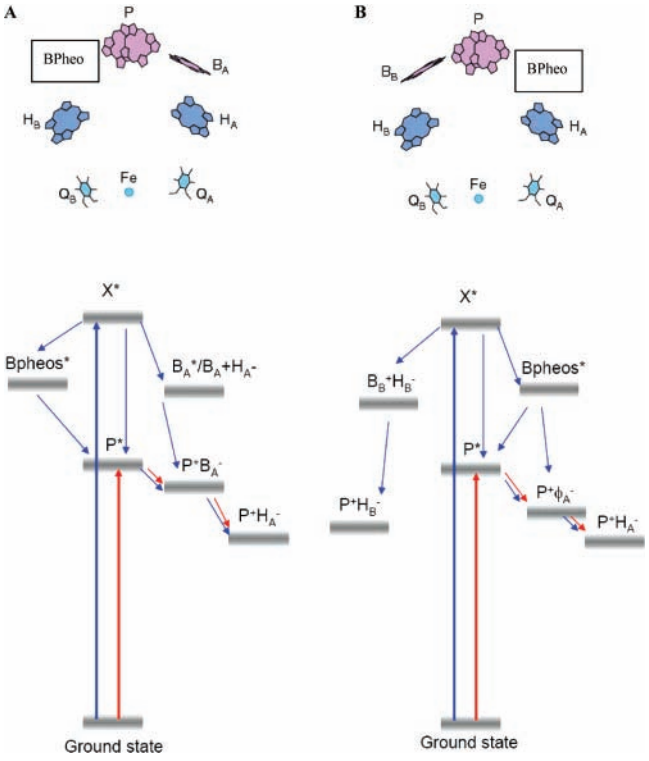

Figure 4. Two models of pigment arrangement and electron-transfer pathways upon different excitations in the *Cf. aurantiacus* RC. The thick red arrows indicate the photon absorption for 865 nm excitation, and the thin red arrows indicate subsequent electron-transfer processes; the blue arrows have the same meaning but for 390 nm excitation.

aurantiacus RC is located on the B-branch, as we proposed in the second model (see below), and therefore senses a weaker electric field due to the formation of $P^+H_A^-$.

The overall charge separation process in the *Cf. aurantiacus* RC has been thought to be similar to that in the *Rb. sphaeroides* RC. However, the most recent research indicates that the primary photochemistry is not quite as simple as originally thought.[38,39] Here, we present additional spectral and kinetic data generated using different excitation wavelengths to further understand the electron-transfer processes in the *Cf. aurantiacus* RC. A comparison of the results obtained under different excitation conditions clearly demonstrates the formation of charge-separated states other than $P^+H_A^-$ (see Figures 2 and 3). Just as in the *Rb. sphaeroides* RC, the route of charge separation strongly depends on the initial wavelength of the excitation and on the energy levels of the intermediates and the specific interactions among cofactors in the RC system.

On the basis of the data from this study, two kinetic models are proposed in accordance with the two possible locations of the monomeric BChl in the *Cf. aurantiacus* RC (Figure 4A and B). In model A, the monomeric BChl is located on the A-branch of the electron-transfer chain (the cofactor is denoted B_A). A charge-separated state $P^+H_A^-$ is formed with a time constant of 7 ps, likely via $P^+B_A^-$ when the P band is excited directly by low-energy photons (the kinetic processes are shown in red arrows). Upon high-energy photon excitation at 390 nm, a higher excited state (X*) is generated, which in principle can (1) relax to P* then form $P^+H_A^-$; (2) produce the excited states of BPheos and BChl, and the excited-state subsequently transfers to P; or (3) form various charge-separated states (for example, $B_A^+H_A^-$) before being stabilized to the $P^+H_A^-$ state. The nanosecond transient spectra with 390 nm excitation also suggests a long-lived state involving BPheos. The only possible states in model A would be $P^+\phi_B^-$ or $P^+H_B^-$, whichever has the BPheo bleaching at 538 nm. In addition, this state exhibits a long-lived 755 nm bleaching (the BPheo Q_Y) that is much stronger than that formed in other states involving BPheo, likely due to the narrow and relatively small absorption increase in the 780−800 nm region. In model B, the monomeric BChl is placed in the B-branch (denoted B_B). In this case, the electron transfer from P to H_A would have to pass ϕ_A, a BPheo at B_A position instead of BChl. The possible weaker electronic coupling between P and ϕ_A could explain the slower electron-transfer rate of 7 ps, as compared with 3 ps in the *Rb. sphaeroides* RC. A similar electron transfer from P to ϕ_B was also observed in the H(M182)L mutant, resulting in a 35% yield of electron transfer to the B-branch.[29] The 390 nm excitation will generate various excited or charge-separated states. In addition to the states listed in model A, a fast formation of $B_B^+H_B^-$ becomes possible, as previously observed in the *Rb. sphaeroides* RC.[31] Because the spectral changes at later times still show the characteristics of BPheo bleachings at 538 and 755 nm, it is reasonable to suggest that the $B_B^+H_B^-$ state evolves to a more stable state $P^+H_B^-$ at later times.

Although it still needs to be verified which model is more realistic by structural data, the observed results clearly show the differences of the electron-transfer processes generated by different excitation in the *Cf. aurantiacus* RC and *Rb. sphaeroides* RC, suggesting a different electron coupling among cofactors in the RCs probably due to the different pigment arrangement on the two branches in addition to the different pigment contents.

Acknowledgment. This work has been supported in part by DOE grant No. DE-FG02-04ER15550 to REB.

References and Notes

(1) Blankenship, R. E. *Molecular Mechanisms of Photosynthesis*; Blackwell Science Inc.: Oxford, UK, 2002.

(2) Blankenship, R. E.; Olson, J. M.; Miller, M. In *Anoxygenic Photosynthetic Bacteria;* Blankenship, R. E., Madigan, M. T., Bauer, C. E., Eds.; Kluwer Academic Publishers: Dordrecht, The Netherlands, 1995; pp 399−442.

(3) Kirmaier, C.; Holten, D.; Feick, R.; Blankenship, R. E. *FEBS Lett.* **1983**, *158*, 73−78.

(4) Blankenship, R. E. *Photochem. Photobiol.* **1984**, *40*, 801−806.

(5) Mimuro, M.; Nozawa, T.; Tamai, N.; Shimada, K.; Yamazaki, I.; Lin, S.; Knox, R. S.; Wittmershaus, B. P.; Brune, D. C.; Blankenship, R. E. *J. Phys. Chem.* **1989**, *93*, 7503−7509.

(6) Causgrove, T. P.; Brune, D. C.; Wang, J.; Wittmershaus, B. P.; Blankenship, R. E. *Photosynth. Res.* **1990**, *26*, 39−48.

(7) Griebenow, K.; Muller, M. G.; Holzwarth, A. R. *Biochim. Biophys. Acta* **1991**, *1059*, 226−232.

(8) Muller, M. G.; Griebenow, G. K.; Holzwarth, A. R. *Biochim. Biophys. Acta* **1993**, *1144*, 161−169.

(9) Ovchinnikov, Y .A.; Abdulaev, N. G.; Zolotarev, A. S.; Shmukler, B. E.; Zargarov, A. A.; Kutuzov, M. A.; Telezhinskaya, I. N; Levina, N. B. *FEBS Lett.* **1988**, *231*, 237−242.

(10) Ovchinnikov, Y. A.; Abdulaev, N. G.; Shmukler, B. E.; Zargarov, A. A.; Kutuzov, M. A.; Telezhinskaya, I. N.; Levina, N. B.; Zolotarev, A. S. *FEBS Lett.* **1988**, *232*, 364−368.

(11) Shiozawa, J. A.; Lottspeich, F.; Oesterhelt, D.; Feick, R. *Eur. J. Biochem.* **1989**, *180*, 75−84.

(12) Zuber, H., Cogdell, R. J. In *Anoxygenic Photosynthetic Bacteria*; Blankenship, R. E., Madigan, M. T., Bauer, C. E., Eds.; Kluwer Academic Publishers: Dordrecht, The Netherlands, 1995; pp 315−348.

(13) Pierson, B. K.; Thornber, J. P. *Proc. Natl. Acad. Sci. U.S.A.* **1983**, *80*, 80−84.

(14) Blankenship, R. E.; Feick, R.; Bruce, B. D.; Kirmaier, C.; Holten, D.; Fuller, R. C. *J. Cell. Biochem.* **1983**, *22*, 251−261.

(15) Yurkova, E. V.; Tsygannik, I. N.; Zargarov, A. G.; Zolotarev, A. S.; Abdulaev, N. G.; Demin, V. V. *FEBS Lett.* **1989**, *256*, 167−169.

(16) Feick, R.; Ertlmaier, A.; Ermler, U. *FEBS Lett.* **1996**, *396*, 161−164.

(17) Shiozawa, J. A.; Lottspeich, F.; Feick, R. *Eur. J. Biochem.* **1987**, *167*, 595−600.

(18) Vasmel, H.; van Dorssen, R. J.; De Vos, G. J.; Amesz, J. *Photosynth. Res.* **1986**, *7*, 281−294.
(19) Bruce, B. D.; Fuller, R. C.; Blankenship, R. E. *Proc. Natl. Acad. Sci. U.S.A.* **1982**, *79*, 6532−6536.
(20) Kirmaier, C.; Holten, D.; Parson, W. W. *Biochim. Biophys. Acta* **1985**, *810*, 33−48.
(21) Kirmaier, C.; Blankenship, R. E.; Holten, D. *Biochim. Biophys. Acta* **1986**, *850*, 275−285.
(22) Volk, M.; Scheidel, G.; Ogrodnik, A.; Feick, R.; Michel-Beyerle, M. E. *Biochim. Biophys. Acta* **1991**, *1058*, 217−224.
(23) Michel-Beyerle, M. E.; Plato, M.; Deisenhofer, J.; Michel, H.; Bixon, M.; Jortner, J. *Biochim. Biophys. Acta* **1988**, *932*, 52.
(24) Vasmel, H.; Amesz, J.; Hoff, A. J. *Biochim. Biophys. Acta* **1986**, *852*, 159.
(25) Parson, W. W.; Chu, Z. T.; Warshel, A. *Biochim. Biophys. Acta* **1990**, *1017*, 251.
(26) Kirmaier, C.; Holten, D. *Photosynth. Res.* **1987**, *13*, 225−260.
(27) Woodbury, N. W.; Allen, J. P. In *Anoxygenic Photosynthetic Bacteria;* Blankenship, R. E., Madigan, M. T., Bauer, C. E., Eds.; Kluwer Academic Publishers: Dordrecht, The Netherlands, 1995; pp 527−557.
(28) Heller, B. A.; Holten, D.; Kirmaier, C. *Science* **1995**, *269*, 940−945.
(29) Katilius, E.; Turanchik, T.; Lin, S.; Taguchi, A. K. W.; Woodbury, N. W. *J. Phys. Chem. B* **1999**, *103*, 7386−7389.
(30) Katilius, E.; Babendure, J. L.; Lin, S.; Woodbury, N. W. *Photosynth. Res.* **2004**, *81*, 165−180.
(31) Lin, S.; Katilius, E.; Haffa, A. L. M.; Taguchi, A. K. W.; Woodbury, N. W. *Biochemistry* **2001**, *40*, 13767−13773.
(32) Sadekar, S.; Raymond, J.; Blankenship, R. E. *Mol. Biol. Evol.* **2006**, *23*, 2001−2007.
(33) Novoderezhkin, V. I.; Taisova, A. S.; Fetisova, Z. G.; Blankenship, R. E.; Savikhin, S.; Buck, D. R.; Struve, W. S. *Biophys. J.* **1998**, *74*, 2069−2075.
(34) Feick, R. G.; Fuller, R. C. *Biochemistry* **1984**, *23*, 3693−3700.
(35) Melkozernov, A. N.; Lin, S.; Blankenship, R. E. *Biochemistry* **2000**, *39*, 1489−1494.
(36) Montano, G. A.; Xin, Y. Y.; Lin, S.; Blankenship, R. E. *J. Phys. Chem. B* **2004**, *108*, 10607−10611.
(37) Becker, M.; Nagarajan, V.; Middendorf, D.; Parson, W. W.; Martin, J. E.; Blankenship, R. E. *Biochim. Biophys. Acta* **1991**, *1057*, 299−312.
(38) Brederode, M. E.; van Grondelle, R. *FEBS Lett.* **1999**, *455*, 1−7.
(39) Van Brederode, M. E.; van Mourik, F.; van Stokkum, I. H. M.; Jones, M. R.; van Grondelle, R. *Proc. Natl. Acad. Sci. U.S.A.* **1997**, *96*, 2054−2059.